Long-Range Attraction and Molecular Rearrangements in Receptor-Ligand Interactions

D. E. LECKBAND, J. N. ISRAELACHVILI, F.-J. SCHMITT, W. KNOLL

A surface force apparatus was used to measure a long-range attractive protein-ligand force at separations D < 85 angstroms. This force may effectively "steer" ligand trajectories, resulting in a greater than 27-fold enhancement of the association rate. A much stronger specific attraction is measured at contact (D < 4 angstroms). A sevenfold increase in intermembrane adhesion resulted from increased lateral mobility of the receptors and molecular rearrangements in membranes above the solid-fluid transition temperature.

IT HAS BEEN PROPOSED THAT LONG-range attractive forces between proteins and ligands steer bimolecular trajectories, influencing association rate constants (*1–4*). Such protein-ligand attractive forces have often been invoked to account for the near diffusion-controlled protein-ligand association rates (*5*). Moreover, computer simulations and mutagenesis studies suggest that long-range intermolecular attractive forces may enhance association rates 30-fold (*2, 3*), but such forces have never been experimentally confirmed. These forces would enhance association rates not only by lowering the potential energy barrier of the collision but also by orienting bimolecular trajectories. With respect to the dynamics of these interactions, receptor mobility and molecular rearrangements on cell surfaces are thought to be important determinants of the strength of cell adhesion, although this was never unequivocably demonstrated (*6–9*).

Until recently, little was known concerning the ranges and magnitudes of these long-range attractive forces. We have used a surface force apparatus (SFA) to make such measurements. The SFA enables the forces between two smooth curved macroscopic surfaces to be measured in a liquid as a function of separation. The force resolution is 10 nN, and distances can be measured to within 1 Å by means of an optical interference technique (*10, 11*). Recent developments in SFA measurements demonstrated that dynamic events, such as molecular rearrangements, can be directly visualized during an experiment (*12*).

We have chosen the well-characterized streptavidin-biotin pair as a model for the direct measurement of protein-ligand intermolecular forces (*13*). Streptavidin, a nonglycosylated homotetrameric protein (molecular weight 60,000) with four biotin binding sites, has a twofold axis of symmetry, and each of two pairs of biotin binding sites lies on each of two faces of the protein (*14*). Oriented membrane-bound monolayers of streptavidin can be easily formed (*14*), and such membrane-associated proteins can also be used to model cell surface receptors. The short-range forces responsible for tight streptavidin-biotin binding are known from crystallographic and chemical modification studies. However, little is known regarding the role of long-range forces in the binding (*15, 16*). The direct measurement of laws that govern streptavidin-biotin interaction forces, therefore, would not only verify the involvement of known interaction forces but, more importantly, would also directly demonstrate whether long-range forces, such as hydrophobic and electrostatic forces, are important in binding and in directing ligand trajectories to the binding pocket.

Biotin and streptavidin were immobilized to supported lipid bilayers (*13*), and the interaction forces were measured as a function of the streptavidin-biotin separation distance D (*10, 13*), in a solution of 0.2 mM sodium phosphate and 0.1 mM NaCl at pH 7.4 and 33°C. At 33°C, the supporting bilayers are in the fluid state [the chain melting temperature T_c of the lipids is 30°C (*17*)]. The position corresponding to $D = 0$ was taken as the position at which the two surfaces achieve strong adhesive contact (Fig. 1). The depth of the minimum, corresponding to the short-range attraction, was determined from the force required to separate the surfaces—the adhesion or pull-off force. At D > 4 Å, the interaction is dominated by an electrostatic double-layer repulsion. At D < 4 Å, a strong short-range attraction was measured that was nearly ten times the typical van der Waals forces measured between fluid lipid bilayers (*11*). The adhesive force is comparable to previous measurements at 33°C, despite the increased pH in these experiments, attesting to its nonelectrostatic origins (*13*).

The specificity of this strong intermembrane adhesion was verified by measurement of the interaction of the biotin surface with biotin-inactived streptavidin prepared by pretreatment with soluble biotin. The resulting force curve together with the force profile between active streptavidin and biotin are shown in Fig. 2. Before the measurements, the streptavidin surface was incubated for 4 hours at 25°C with soluble biotin at 10^{-7} M in 1 mM NaCl and pH 5.6. After the incubation, the surface was rinsed with 700 ml of 1 mM NaCl and remounted in the apparatus. Curve a was then measured between inactive streptavidin and biotin surfaces under conditions identical to those used in the measurements of active streptavidin and biotin interactions. Curve b is the interaction force profile of active streptavidin and biotin surfaces under the same conditions as for curve a, except that the streptavidin was not inactivated before the measurement. The solid line through the data is a least squares fit to a simple exponential function, $F/R = (F/R)_0 e^{-D/\lambda}$, where $(F/R)_0$ is the maximum extrapolated repulsion at contact and λ is the decay length of the long-range repulsion. The best fit parameters were $(F/R)_0$ = 1.2 mN/m and λ = 105 Å. A comparison of curve a with curve b shows that the long-range electrostatic repulsion measured with active streptavidin (curve b) is reduced relative to curve a. Taking the difference between curves a and

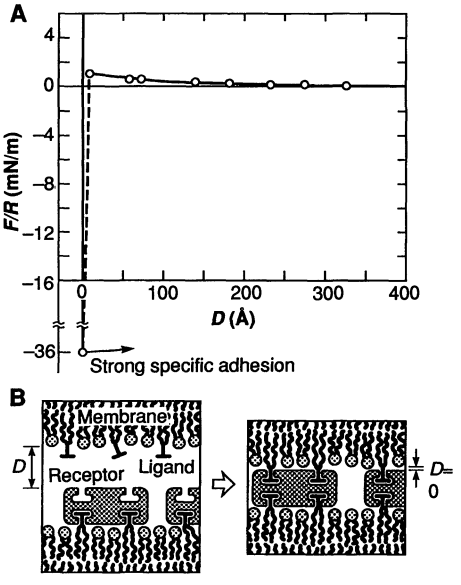

Fig. 1. (**A**) Force profile for the interaction of streptavidin with 5% biotin (plotted as the force F, normalized by the radius of curvature of the surfaces R, against surface separation D). The streptavidin-biotin interaction force profile was measured at pH 7.4 and 33°C (0.3 mM Na^+). The long-range interaction (D > 4 Å) was typical of interacting charged surfaces, and the double-layer electrostatic force was well described by an exponential decay. At separations D < 4 Å, the surfaces experienced a strongly adhesive force, nearly ten times the typical van der Waals forces. (**B**) Schematic showing the ligand-receptor binding.

D. E. Leckband and J. N. Israelachvili, Department of Chemical and Nuclear Engineering, University of California, Santa Barbara, CA 93106.
F.-J. Schmitt and W. Knoll, Max Planck Institüt für Polymerforschung, Ackermannweg 10, D-6500 Mainz, Germany.

b (curve c), one can attribute the difference in the measured force profiles to an additional attractive force at $D < 85$ Å between active streptavidin and biotin. The exponential distance dependence of this attractive force is shown in Fig. 3.

The absence of the additional long-range attraction in curve a is attributed to the screening of the streptavidin forces at the active sites by the bound biotin because biotin is not expected to alter the electrostatic properties of the streptavidin surface (*18*). This long-range attraction cannot be attributed to electrostatic or van der Waals forces, because the electrostatic forces are identical at $D > 85$ Å and the magnitude and range of the additional attraction are much larger than those of any possible van der Waals interaction (*19*). In contrast, the range (85 Å) and decay length (17 Å) are similar to previously measured forces between hydrocarbon surfaces in water (*20–22*); consequently, this force is attributed to the hydrophobic interaction between the exposed hydrophobic surfaces of the biotin and streptavidin binding sites.

These measured biotin-streptavidin interaction forces are consistent with the results of crystallographic and chemical modification studies that indicate a large number of streptavidin-biotin hydrogen bonds, van der Waals contacts, and hydrophobic interactions (*15, 16, 18*). Crystallographic information, however, cannot predict or quantify any long-range streptavidin-biotin interaction force profile. The force measurements, however, demonstrate the significance of such forces in ligand reactivity, particularly in regard to their role in steering bimolecular trajectories.

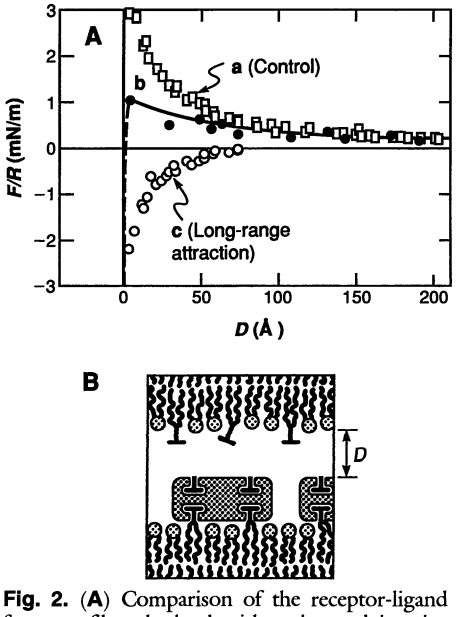

Fig. 2. (**A**) Comparison of the receptor-ligand force profiles obtained with active and inactive streptavidin. Curve a shows the interaction force law measured between biotin-inactivated streptavidin and biotin at pH 7.4 and 33°C. Curve b shows the measured force law between active streptavidin and biotin (compare with Fig. 1) under the same conditions as in curve a. Curve c shows the additional attractive force obtained from the difference between curves a and b. (**B**) Schematic depiction of the control experiment.

The data of Fig. 2 allow us to estimate the effect of the increased long-range attraction (equivalent to a reduced repulsion) on enzyme-surface collision rates. The relative rates are approximately (*23*)

$$k_1/k_2 = \exp(-\Delta E/kT)$$

where k is the Boltzmann constant and T is temperature. We obtained the magnitude of ΔE by taking the difference of the integrated normalized force curves a and b, since

$$E/R = -\int [F(D)/R]\, dD$$

If the forces are assumed to be additive and the protein surface coverage is the same for all radii, the interaction energy between two spheres scales with their radii, R (*19*). Thus, if we assume an enzyme radius of 28 Å, the reduced force barrier of $\Delta F/R = 2$ mN/m at $D = 4$ Å between two macroscopic surfaces of radius R (Fig. 2) corresponds to a reduced energy barrier of $\Delta E \approx 1.4 \times 10^{-20}$ J, which is about 3.3 kT between two microscopic surfaces of radius 28 Å. This would enhance the association rate by a factor of $e^{3.3} \approx 27$. Because the coverage of the protein surface was only 66% in these experiments (*14*), the actual enhancement is expected to be larger and closer to $e^{3.3/0.66} \approx 150$.

In order to investigate the effects of surface mobility on receptor recognition and adhesion, we controlled the lateral mobility of the receptor (streptavidin) by raising or lowering the temperature above or below the solid-liquid transition temperature [$T_c = 30$°C (*17*)] of the lipids in the supporting bilayer. Streptavidin and biotin surfaces and the bathing solution were prepared as described above. Below this transition temperature, the lateral diffusion of surface molecules is restricted ($<10^{-12}$ cm^2/s), whereas, above the transition temperature, diffusion coefficients of the order of 10^{-11} to 10^{-9} cm^2/s are expected (*6, 8*). Consequently, below 30°C, streptavidin-biotin mismatches on opposing membranes have insufficient mobility to adopt favorable orientations, and fewer bonds would form with a subsequent reduction in adhesion. Shown in Fig. 4 are two separate force curves measured at 25°C ($T < T_c$) and 33°C ($T > T_c$). Although the forces at both temperatures are similar, the final adhesion at "contact" is nearly an order of magnitude greater above the chain melting temperature: namely, the intermembrane adhesive strength measured at 33°C was −36 mN/m, but at 25°C the adhesion decreased to −5 mN/m. This effect was reversible. Furthermore, a steric force was measured at a separation ($D < 20$ Å) consistent with the size of the biotin head group (~16 Å) (*24*). This short-range steric repulsive force is associated with a biotin configurational reorientation that takes place before the binding of the streptavidin. As the molecules diffuse on the surface, the biotins bind streptavidin or orient parallel to the surface, and the force is abolished.

Significantly, this short-range steric interaction was time-dependent: if at 33°C the surfaces were brought together sufficiently slowly (less than 1 Å/s) to allow for molecular reorientations, the steric force was unobserved (Fig. 1). If, however, the full compression was carried out much faster, the steric force was observed. However, if the surfaces were brought together quickly but then allowed to relax or equilibrate near the repulsive maximum (at $D = 65$ Å), this force collapsed within 15 s. In contrast, at 25°C, where molecular lateral motion is

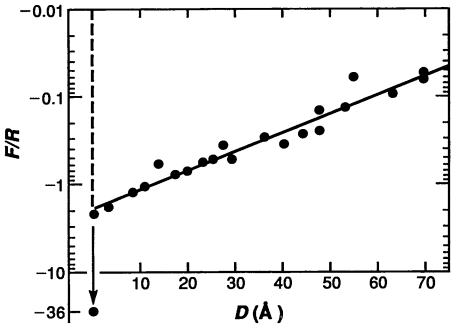

Fig. 3. Logarithmic dependence of the long-range streptavidin-biotin attractive force. The long-range attractive force of Fig. 2, curve c, plotted on a logarithmic scale. A least squares fit of the function $F/R = (F/R)_0 e^{-D/\lambda}$ to the data yields $(F/R)_0 = -2.5$ mN/m and $\lambda = 17$ Å.

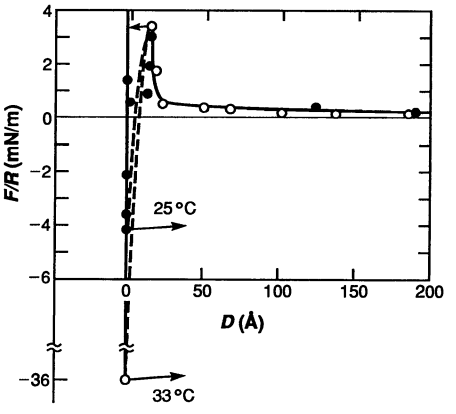

Fig. 4. Dependence of the specific intermembrane adhesion on the fluidity of the supporting bilayer. The interaction and adhesion forces between 5% biotin and streptavidin surfaces measured at 25°C (●) and 33°C (○) at pH 7.4 (0.3 mM Na^+).

limited and surface molecules have insufficient time to form complementary alignments on opposing membranes, the steric force was always observed. Consequently, these observed molecular rearrangements can be directly correlated to the lateral mobility of the receptor and the resulting increase in intermembrane adhesion, demonstrating the importance of surface mobility in the strength of cell adhesion.

REFERENCES AND NOTES

1. S. A. Allison, G. Ganti, J. A. McCammon, *Biopolymers* **24**, 1323 (1985).
2. P. Slayton and S. Sligar, *Biochemistry* **29**, 7381 (1990).
3. J. J. Wendoloski, J. B. Matthew, P. C. Weber, F. R. Salemme, *Science* **238**, 794 (1987).
4. E. Margoliash and H. R. Bosshard, *Trends. Biochem. Sci.* **8**, 316 (1983).
5. T. E. Creighton, *Proteins* (Freeman, New York, 1989), p. 340.
6. F. W. Wiegel, in *Cell Surface Dynamics*, A. S. Perelson, C. DeLisi, F. W. Wiegel, Eds. (Dekker, New York, 1984), chap. 5.
7. P. Bongrand and G. Bell, *ibid.*, chap. 14.
8. G. Bell, in *Physical Basis of Cell-Cell Adhesion* (CRC Press, Boca Raton, FL, 1988), chap. 10.
9. E. Evans, *Biophys. J.* **48**, 185 (1985).
10. J. Marra and J. Israelachvili, *Methods Enzymol.* **127**, 353 (1986).
11. J. Marra, *Biochemistry* **24**, 4608 (1985).
12. D. E. Leckband, C. Helm, J. Israelachvili, unpublished results.
13. C. A. Helm, W. Knoll, J. N. Israelachvili, *Proc. Natl. Acad. Sci. U.S.A.* **88**, 8169 (1991).
14. R. Blankenburg, P. Meller, H. Ringsdorf, C. Salesse, *Biochemistry* **28**, 8214 (1989).
15. M. Green, *Adv. Protein Chem.* **29**, 85 (1975).
16. E. Bayer and M. Wilchek, *Methods Enzymol.* **184**, 49 (1990).
17. G. Cevc and D. Marsh, *Phospholipid Bilayers: Physical Principles and Models* (Wiley, New York, 1984), p. 242.
18. W. A. Hendrickson *et al.*, *Proc. Natl. Acad. Sci. U.S.A.* **86**, 2190 (1989).
19. J. Israelachvili, *Intermolecular and Surface Forces* (Academic Press, New York, ed. 1, 1985), chap. 11.
20. H. K. Christenson and P. M. Claesson, *Science* **239**, 390 (1988).
21. P. Claesson, P. Herder, J. Berg, H. Christenson, *J. Colloid Interface Sci.* **136**, 541 (1990).
22. J. Israelachvili and R. Pashley, *Nature* **300**, 341 (1982).
23. R. S. Berry, S. A. Rice, J. Ross, *Physical Chemistry* (Wiley, New York, 1980), pp. 1160–1165.
24. D. E. Metzler, *Biochemistry* (Academic Press, New York, 1977), p. 433.

25. We thank H. Ringsdorf, W. Muller, and E. Rump for valuable discussions. D.E.L. was supported by NIH grant GM13300, and funding was provided by NSF grant CTS-9015537.

28 October 1991; accepted 27 January 1992

A Mass Transfer Explanation of Metabolic Scaling Relations in Some Aquatic Invertebrates and Algae

MARK R. PATTERSON

Chemical engineering theory can be used in accounting for the broad range of metabolic scaling exponents found in some aquatic invertebrates and algae. Delivery of metabolically important compounds to these organisms occurs by diffusion through a boundary layer. Dimensionless relations (Sherwood-Reynolds number functions) demonstrate the degree to which water motion and organism size affect mass transfer, and ultimately, metabolic rate. Derivation of mass exponents in the range 0.31 to 1.25 for simple geometries such as plates, spheres, and cylinders directly follows from knowledge of the Sherwood-Reynolds number relations. The range of exponents predicted is that found by allometric studies of metabolic rate in these organisms.

THE RELATION BETWEEN BODY SIZE and metabolic rate in organisms is a subject of great interest to physiologists and ecologists because many organisms increase in size by one to several orders of magnitude during ontogeny, and life on Earth spans 19 orders of magnitude in mass (*1*). The relation between organism mass (M) and metabolic rate (R) is nonlinear and usually described by a power-law function: $R = aM^b$, where a is termed the mass coefficient and b the mass exponent (*2*). The nature of the allometric relation between metabolic rate and body size in homeotherms has been intensively examined (*3*). Many explanations for the clustering of interspecific mass exponents around a value of 0.75 (Kleiber's Rule) have been offered (*4*) although there is disagreement as to whether the data support the 3/4 power law or a mass exponent statistically indistinguishable from 0.67 (*5*). The situation for some aquatic invertebrates and algae is less well examined or understood. Mass exponents range from 0.47 to 1.28, with no obvious clustering around 0.75 or 0.67 [Table 1; (*6*)]. These empirical observations provoke the question of why there is such large variation in mass exponent in these taxa.

Many lower aquatic organisms have been shown to be sensitive to the rate of fluid mixing near their exchange surfaces (*7*). Such organisms are usually oxyconformers that lack mechanisms for active ventilation of exchange surfaces. They are dependent on diffusion through a boundary layer (*8*) for uptake of metabolically important compounds such as oxygen, and in the case of photosynthetic organisms or symbiotic associations, bicarbonate ion–carbon dioxide. A particularly powerful means of examining flow effects on metabolic rate is to make both the fluid convection and metabolic rate dimensionless by use of the Reynolds number and the Sherwood number (*9*). The Reynolds number ($\mathrm{Re} = \rho UW/\mu$) expresses the ratio of inertial forces to viscous forces that govern fluid motion around an organism, where ρ is fluid density [dimensions: mass (M) length $(L)^{-3}$], μ is dynamic viscosity [mass (M) length $(L)^{-1}$ time $(T)^{-1}$], W is organism characteristic dimension (L), and U is flow speed ($L\ T^{-1}$). The Sherwood number ($\mathrm{Sh} = h_m W/D$) is a dimensionless index of metabolism; it is the ratio of mass transfer assisted by fluid motion to that which would occur if diffusion through a still layer of fluid was the only mechanism of transport to the organism, where h_m is the mass transfer coefficient ($L\ T^{-1}$), and D is the diffusion coefficient of the dissolved species [$L^2\ T^{-1}$; (*10*)].

Plots of Sh (ordinate) – Re (abscissa) yield information on the degree to which water motion affects mass transfer (*11*). The relation is often expressed as a power law ($\mathrm{Sh} = c\mathrm{Re}^d$). Flow-size exponents ($d$) range from 0.5, for mass transfer through a laminar boundary layer, to greater than 0.8, for transfer through a turbulent boundary layer (*11*). This mode of analysis has been infrequently applied to aquatic organisms, but flow exponents consistent with both laminar and turbulent boundary layer transfer have been observed for cnidarians (*9*). Because organism size affects Re, and Re affects metabolic rate (disguised as Sh), it is possible to examine the consequences of size in aquatic organisms where this sort of physicochemical regulation of metabolic rate obtains (Fig. 1).

I made theoretical predictions of metabolic scaling for organisms possessing some simple geometries of uptake surface (flat plate, sphere, and cylinder) subject to assumptions of laminar or turbulent flow in the organismic boundary layer (Table 2). These geometries were chosen because many aquatic invertebrates and algae have similar shapes. Solving the simultaneous equations $\mathrm{Re} = \rho/UW/\mu$, $\mathrm{Sh} = c\mathrm{Re}^d$, and $\mathrm{Sh} = h_m W/D$, for h_m (*12*) gives

$$h_m = \frac{c\,D\,W^{d-1}\,\rho^d\,U^d}{\mu^d} \qquad (1)$$

Substituting for h_m in the generalized flux (metabolic) equation (*11*) and simplifying

Division of Environmental Studies, University of California, Davis, CA 95616.